BEAM DETECTOR

By

O. Kraus

Internal Memorandum
M Report No. 264
May 1961

W. W. Hansen Laboratories
Stanford University
Stanford, California

TABLE OF CONTENTS

LIST OF FIGURES

BEAM DETECTOR

1. METHOD OF DETECTION

The purpose of the device described below is to measure the intensity of the electron beam in the accelerator and its possible deviation from the normally axial position.

Besides the various intercepting devices for beam intensity measurement, only one nonintercepting instrument is in actual use. It employs a toroidal coil wound on a suitable core and placed around the beam.

The new instrument, to be illustrated below, employs no coils. Instead, it employs pairs of loops of very small dimensions located inside the beam-carrying pipe, very close to its walls and relatively far from the beam. With four loops placed in symmetrical and diametrically opposite positions, both the position of the beam and its intensity can be determined. The field distortion introduced by such loops in a waveguide-type microwave structure is similar to the distortion caused by the usual loop-type probes used in VSWR measurements; i.e., the field distortion is a minimum if the probes are not deeply introduced into the field.

An additional favorable factor is that in the particular case of the tests we have performed, and of the possible future uses of the instrument in connection with the accelerator, the loops are introduced in interconnecting structures between successive sections; i.e., in beam-drift spaces. These beam-drift spaces carry no actual microwave power, in the ordinary sense of this expression, but only a highly attenuated S-band field created in loco and fields pertaining to harmonics. All of these are produced by the electron bunches, i.e., as components of their Fourier-type representation. The 10.5 cm distance between successive electron bunches accounts for the presence of the 2856 Mc/sec fundamental frequency.

From the point of view of the beam intensity measurement the small loops placed inside the drift space, with their planes oriented as the axis of the pipe, represent as many turns of a virtual coil as there are loops. The difference between the turns of a coil and the loops is that, while the emf induced by the beam in each turn of a

coil is added in the coil itself, quantities proportional to the emf's induced in the various loops are summed only after some prior manipulation. The advantage is that the loop-emf's are proportional both to the beam intensity and to its position with respect to the loops. Hence, the beam position can be deduced.

2. CALCULATION OF THE LOOP SIGNALS

The electron bunches in transit through the drift space can be represented as a charge distribution along the pipe axis. The latter is both a space and time axis. We can consider a number of bunches, as many as the drift space can contain, as frozen in a suitable position. Although in Fig. 1a these bunches have been represented in a square-like form, this fact has little bearing on the Fourier analysis mentioned above. As a matter of fact, the ratio t/T (see Fig. 1a) is the factor which has the most influence in this latter respect.

A loop placed in the drift space will pick up a composite signal as is given by the Fourier series. For purposes of calculation of this signal, it is necessary to take into account the contributions of each component. This is not an easy task. The drift space has widely different attitudes toward different harmonics. Furthermore, the exact equivalent circuit of the loop and its external load should be adequately represented. The following qualitative consideration can be made relative to a simplified case.

Suppose that the loop feeds an S-band cavity. In such case the other components are of little or no interest. The fundamental component is a virtual beam current of constant amplitude (see Fig. 1b), but from the loop it is seen as a strongly attenuated wave. The attenuation is caused by the drift space diameter which is below the critical value. For this reason, the actual inducing current waveshape has a configuration as in Fig. 1c.

A second approach to this problem, in some way connected to the above considerations, is to examine the effect of two of the bunches out of all those existing at any particular time in the drift space. These two bunches are those located nearest around the loop. The charges represented by the bunches, while moving in front of the loop, could be regarded as a dipole fed by a pulsating, instead of the usual sinusoidal, current.

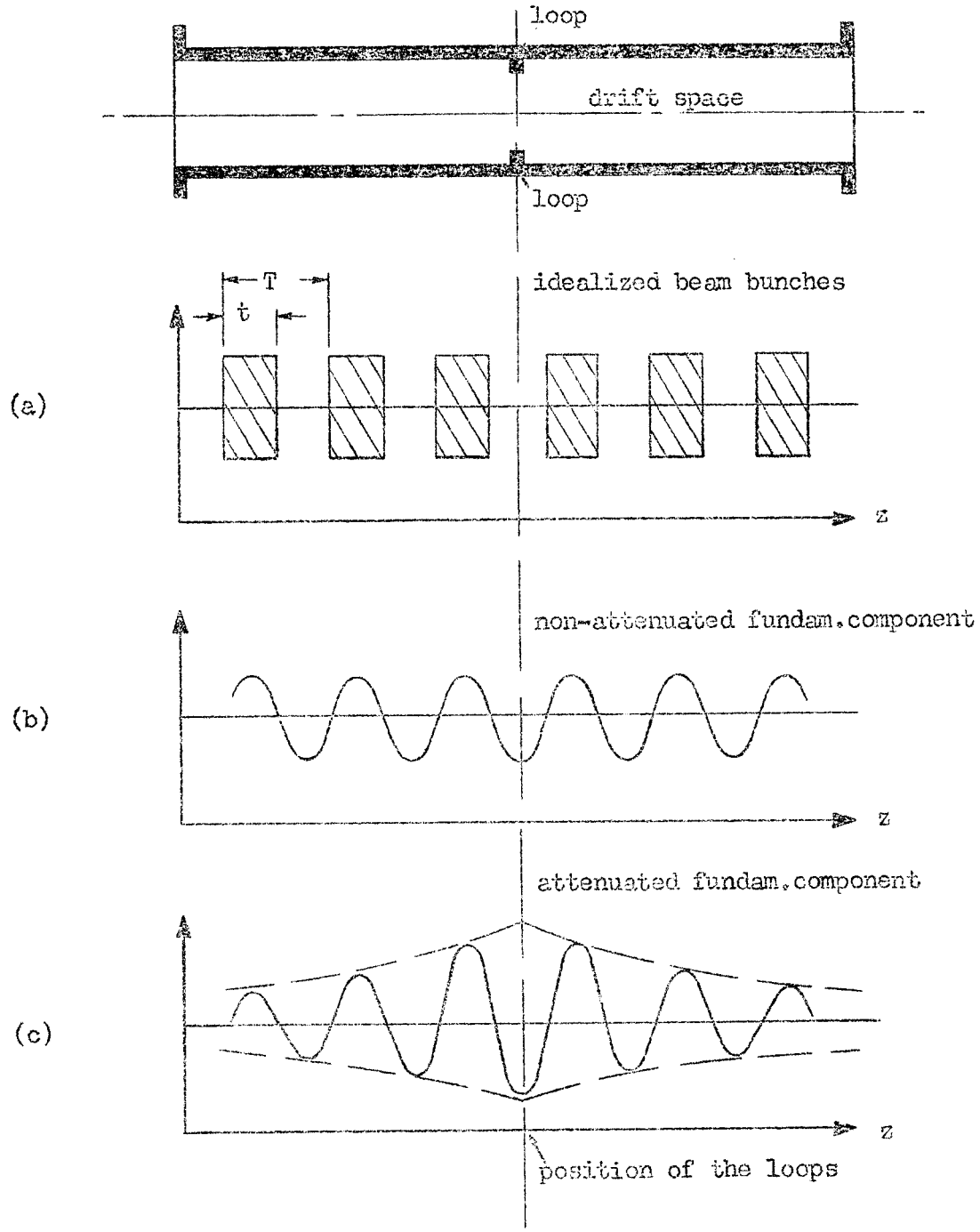

Fig. 1--Waveforms in the drift space.

The origin of these difficulties lies in the fact that the general expression of the electric and magnetic fields is sought. The quantity of real interest is the ratio of the emf's induced in opposite loops. By calculating these emf's, much of the difficulty can be bypassed.

In view of the use of loops, the magnetic field has predominant influence. If it is considered alone, and the electric field and the effect of the walls omitted, an error is introduced; however, in spite of this, useful information can be obtained.

The energy content of a magnetic field established in a volume v is

$$W = \frac{1}{8\pi}\int_v H^2 \, dv \qquad \text{(c.g.s. units)} \tag{1}$$

Essentially, only the fundamental component I_{B1} of the magnetic field created by the beam current I_B is of interest. It is

$$H_1 = \frac{I_{B1}}{2\pi r} \tag{2}$$

at a distance r from the beam. Hence the energy is

$$W_1 = \frac{1}{8\pi}\int_v \frac{I_{B1}^2}{(2\pi r)^2} \, dv \tag{3}$$

With reference to Fig. 2, in which the cross section of the drift space is represented and the beam is supposed to be displaced from point O to a point P, Eq. (3) can be written

$$W_1 = \frac{1}{8\pi}\int_{R_1}^{R_{01}} \frac{I_{B1}^2}{(2\pi r)^2} \, 2\pi r \ell \, dr = \frac{I_{B1}^2 \ell}{16\pi^2}\int_{R_1}^{R_{01}} \frac{dr}{r} \tag{4}$$

where ℓ is the axial dimension of the loop and R_1 and R_{01} are defined in Fig. 2. It results in

$$W_1 = \frac{I_{B1}^2 \ell}{16\pi^2} \log_e \frac{R_{01}}{R_1} \tag{5}$$

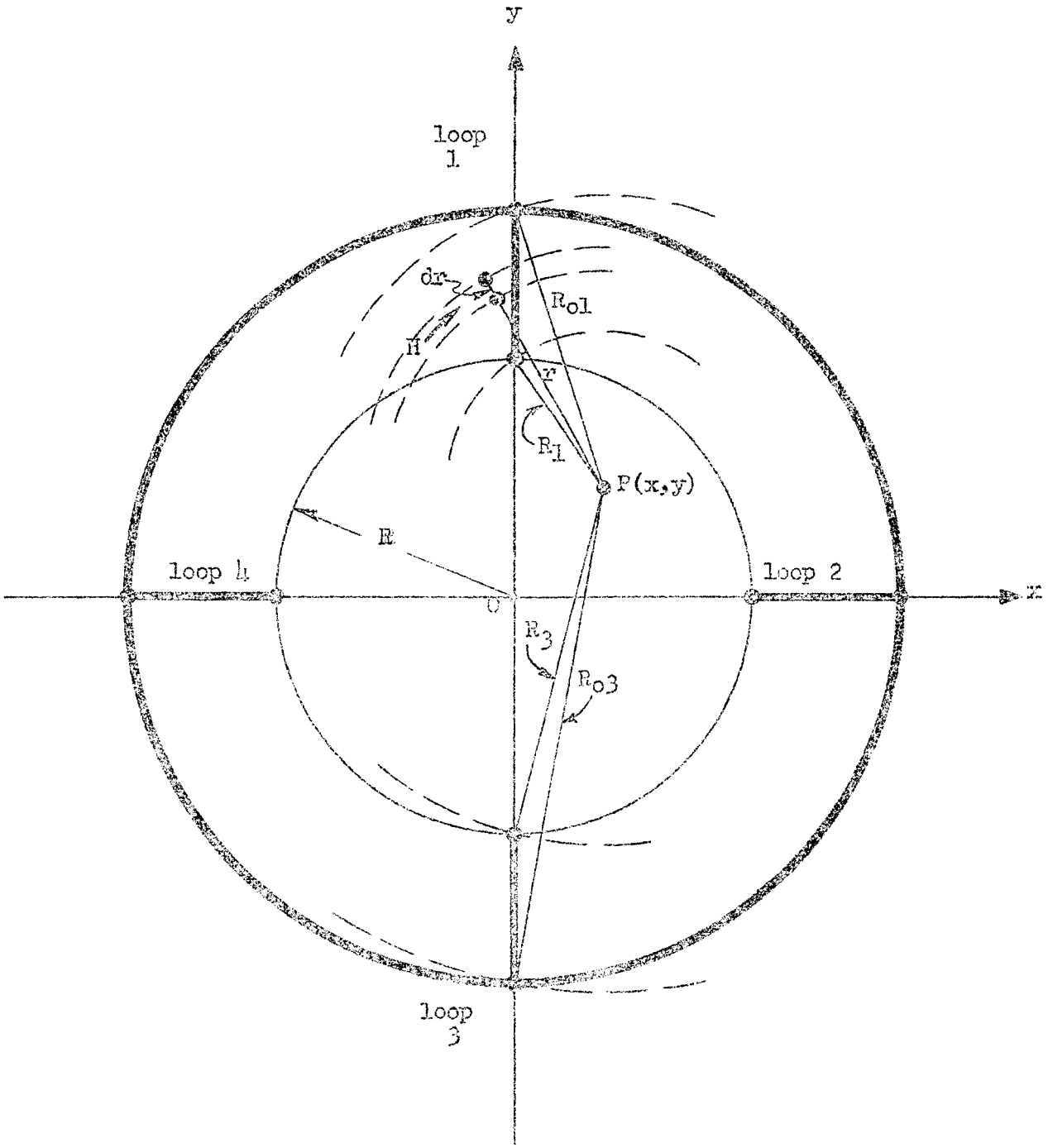

Fig. 2--Cross section of the drift space.

An expansion of $\log_e R_{01}/R_1$ and some approximation yields

$$W_1 = \frac{I_{B1}^2 \ell}{16\pi}\left(\frac{R_{01}^2}{R_1^2} - 1\right) \tag{6}$$

Again with reference to the Fig. 2, Eq. (6) can be written in a different form by geometrically interpreting the meaning of

$$\frac{R_{01}}{R_1^2} - 1 = \frac{1}{4\pi R_1^2}\left(4\pi R_{01}^2 \ell - 4\pi R_1^2 \ell\right) \tag{7}$$

as $1/4\pi R_1^2$ times the volume of the cylindrical pipe, the base of which has internal radius R_1, external radius R_{01}, and height ℓ. Therefore, the magnetic energy contents of the toroid with center in P and flowing through loop 1 is

$$W_1 = \frac{I_{B1}^2}{(4\pi)^3} \frac{\Delta v_1}{R_1^2} \tag{8}$$

where Δv_1 is said volume. Equation (8) is the total energy content of the magnetic field linked with the loop. A fraction η of this energy is actually absorbed by the loop.

The ratio of the energies absorbed by two opposite loops, distinguished by subscripts 1 and 3, of equal characteristics and identically loaded, is therefore

$$\frac{W_1}{W_3} = \frac{R_3^2}{R_1^2} \frac{\Delta v_1}{\Delta v_3} \tag{9}$$

The ratio $\Delta v_1/\Delta v_3$ is linked to the radial dimension w (width) of the rectangular loops and to the radius R of the drift space by

$$\frac{\Delta v_1}{\Delta v_3} = \frac{1 + \frac{2R_1}{w}}{\frac{2}{w}(2R - R_1) - 3} \tag{10}$$

The ratio of the powers P_1 and P_3 absorbed by the two loops has the same value, Eq. (9), and the ratio of the emf's induced in two opposite loops is given by

$$\frac{V_1}{V_3} = \sqrt{\frac{P_1}{P_3}} = \frac{R_3}{R_1}\sqrt{\frac{\Delta v_1}{\Delta v_3}} \tag{11}$$

Figure 3 represents the sensitivity of the system of measurement, defined as

$$S = \frac{P_1 - P_3}{P_1 + P_3} \tag{12}$$

the ratio of the difference of power induced in the two loops to the total power extracted by them from the beam.

3. MEASUREMENT CIRCUIT

Basically, two opposite loop pairs placed at a right angle in the drift space were used for beam position detection. Considering, again, only one pair of such loops, the signals picked up by them were coupled into transmission type cavities tuned to 2856 Mc/sec (see Fig. 4). These are not essential parts of the circuit, primarily being used to select the fundamental component of the loop signal and to achieve some possible additional gain through impedance transformation. A crystal detects the cavity signal. This latter is then amplified by means of a broadband amplifier. The output of this amplifier is the video envelope of the 2856 Mc/sec signal; i.e., a pulse modified in its form, being the "carrier pulse" deprived of its higher harmonic contents. In some of the tests to be described in the next section, the cavity was not used so that the unmodified video pulse was available at the amplifier output. Here, two such cavity-crystal-amplifier channels were used, one for each of the two opposite loops. Each of them is virtually a branch of a bridge, the two other arms being ohmic resistors. Each channel is actually completed by circuit elements ("pulse conditioners"), the function of which is to translate the amplitude of the video signal into a linearly proportional variable resistance represented in its practical form by one triode for

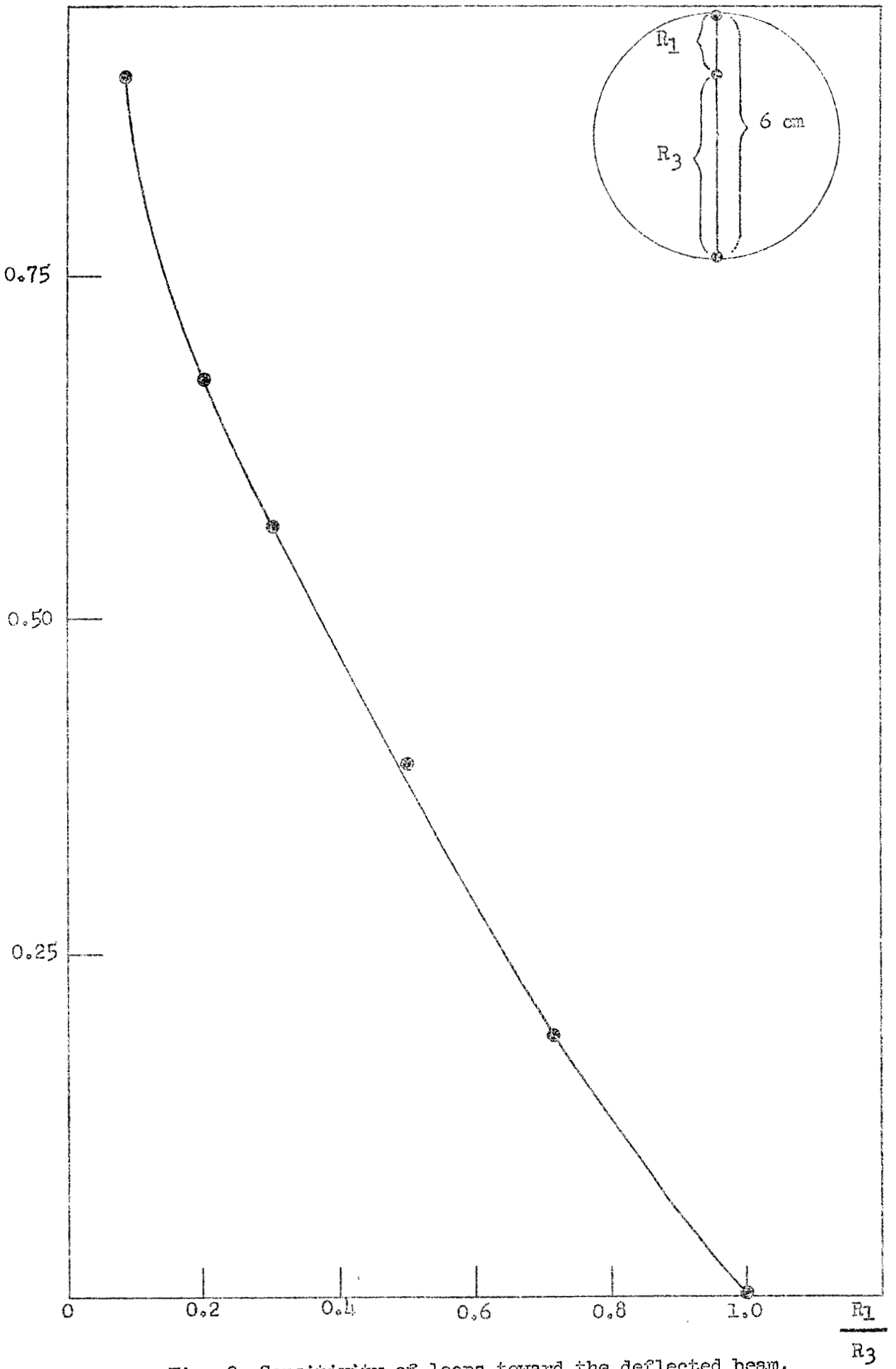

Fig. 3--Sensitivity of loops toward the deflected beam.

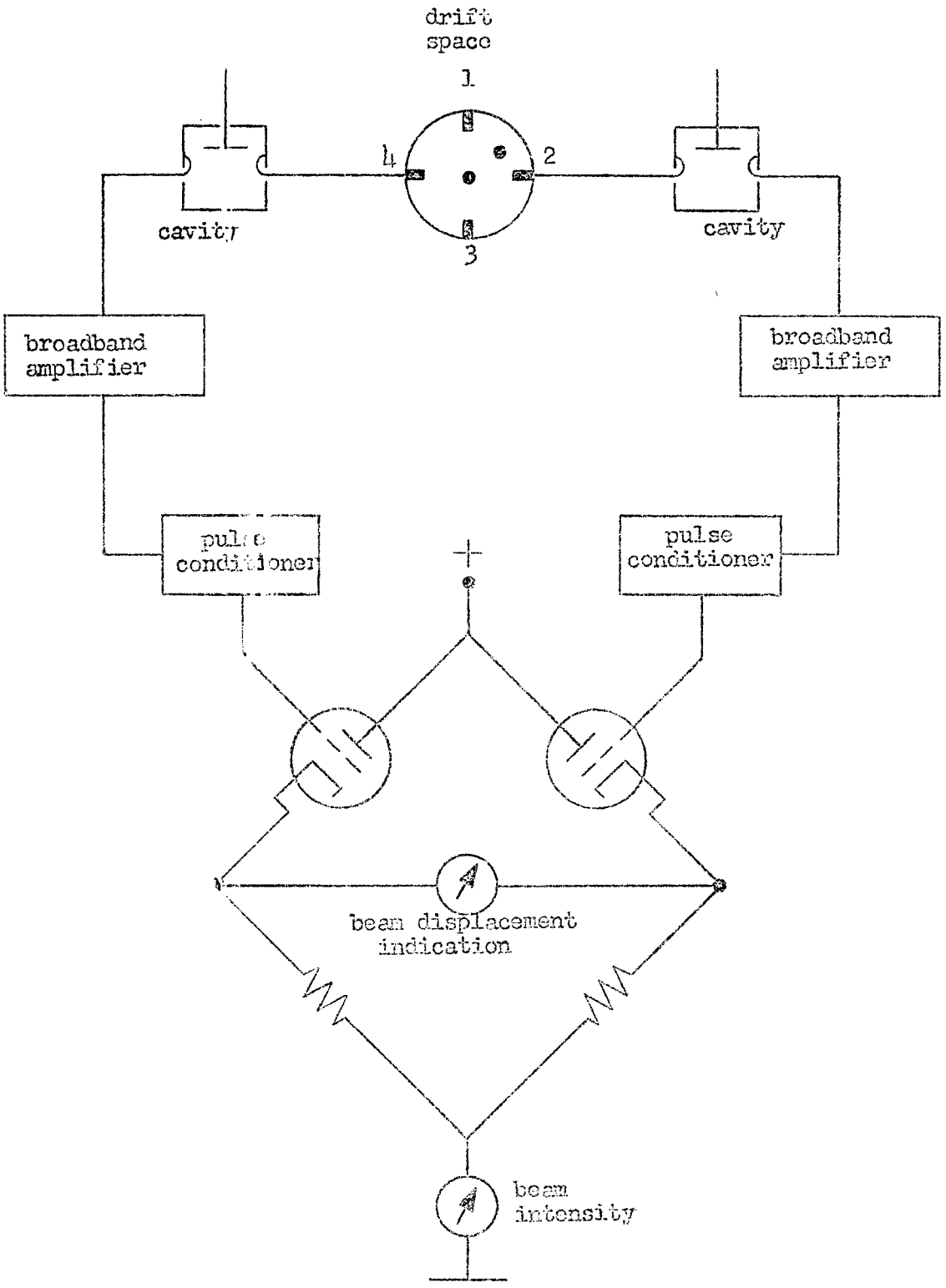

Fig. 4--Beam detector circuit.

each channel. The bridge unbalance is proportional to the beam coordinate along an axis connecting the two loops. As a matter of fact, from Fig. 2

$$R_3^2 - R_1^2 = 4Ry \tag{13}$$

with y ordinate of point P. On the other hand, according to Eq. (9) applied to the absorbed powers, it is approximately

$$P_1 = \frac{k}{R_1^2} \quad \text{and} \quad P_3 = \frac{k}{R_3^2} \tag{14}$$

with k nearly constant. As a result

$$P_1 - P_3 = \frac{4Rk}{R_1^2}\, y \tag{15}$$

and an analogous formula links the abscissa x to the difference $P_2 - P_4$ of the powers absorbed by the loops placed in a horizontal plane. In the specific case of Fig. 4, the indication of the bridge galvanometer is proportional to $P_2 - P_4$ and thus to x.

While the first couple of loops and the relative circuitry supply information relative to the position of the beam in their plane, the other two loops and their circuits serve the same purpose in relation to the beam position in the plane of which they are part. Thus, the system described measures the coordinates of the beam in that cross section of the drift space which contains the axis of the two loops.

4. PRELIMINARY TEST RESULTS: CRYSTAL NONLINEARITY

The few tests performed and the results obtained before the dismantling of Mark IV cannot be considered as final. Repeated and refined tests have to be made before a final word can be said about the system described. Thus, the following data are only indicative.

With an experimental setup like the one represented in Fig. 4 two different tests were run. In both cases the beam was extracted at the accelerator target and passed through an immediately adjacent 15-in. long pipe having a diameter well under the cutoff dimension. Two such pipes, representing the drift space, were alternately used: one entirely open and so under atmospheric pressure, and a second in which the pressure was

around 10^{-4} to 10^{-5} mm Hg. The loops were placed near the target end of the accelerator in order to avoid too much scattering before the beam reached them. The loops were of the usual probe type with a diameter of about 4 mm. The beam current was measured with a Faraday cup used as a reference.

In a first case the beam was gradually deflected by means of the steering coils. While a slight deflection did not cause any substantial variation in the beam current intensity, with increasing deflection more and more current was intercepted by the accelerator structure. In a sense this is the normal way of operation of the accelerator, although if means are provided for the correction of the beam position, the intensity as measured at the target (or at some intermediate point, such as the sector ends) will never vary beyond allowed limits. In any case, in order to eliminate the effect of a varying beam intensity, in a first test this latter was restored to its initial value by adjusting the gun. Therefore, the beam current was constant in the section containing the loops.

While deflecting the beam, both the indications of the beam detector and the amplitude of the video signals into it were rated. This latter was done by means of a dual-channel oscilloscope (although the measurement of amplitudes of irregular pulses with an oscilloscope is a very roughly approximate procedure). In Fig. 5, the various quantities are represented as a function of the steering current:

1. The pulse amplitudes, as visually detected at the oscilloscope. These have a quadratic-like aspect, due mainly to the crystal characteristics.

2. The corresponding bridge indications of the accelerator beam deflection. The relative curve has a clearly linear shape.

While the restored beam current has a constant value (1.2 microamperes in the case of this test), the unrestored beam current has an irregular shape. The truly interesting result is the linearity of the beam deflection indication supplied by the circuit under test. For more exact results, a digital voltmeter was used by means of which the steering current was measured.

During a second test run the beam intensity was not restored, so that the gradual interception of it by the accelerator structure at both sides is clearly visible (see Fig. 6).

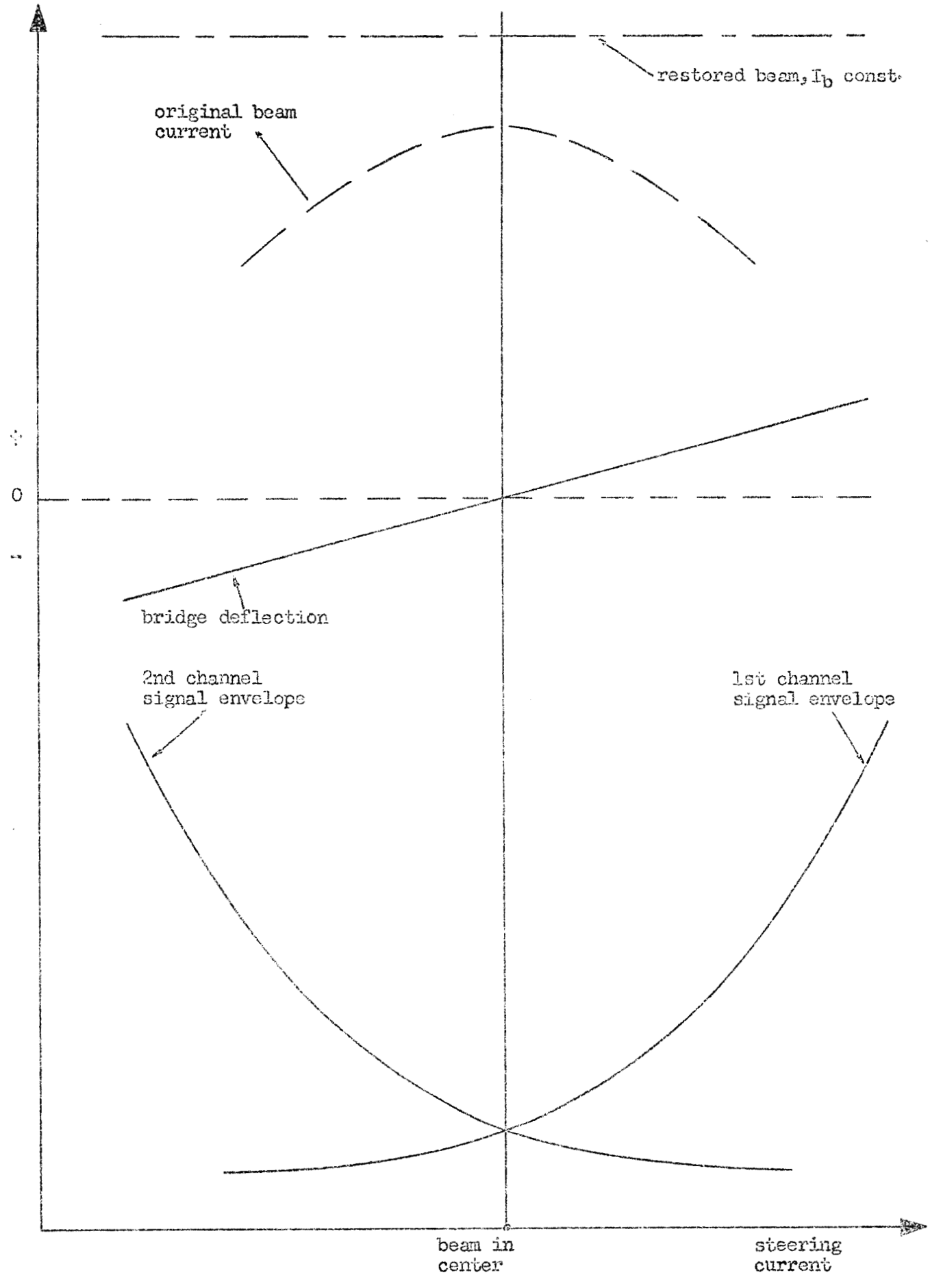

Fig. 5--Beam detector characteristics in case of constant beam intensity.

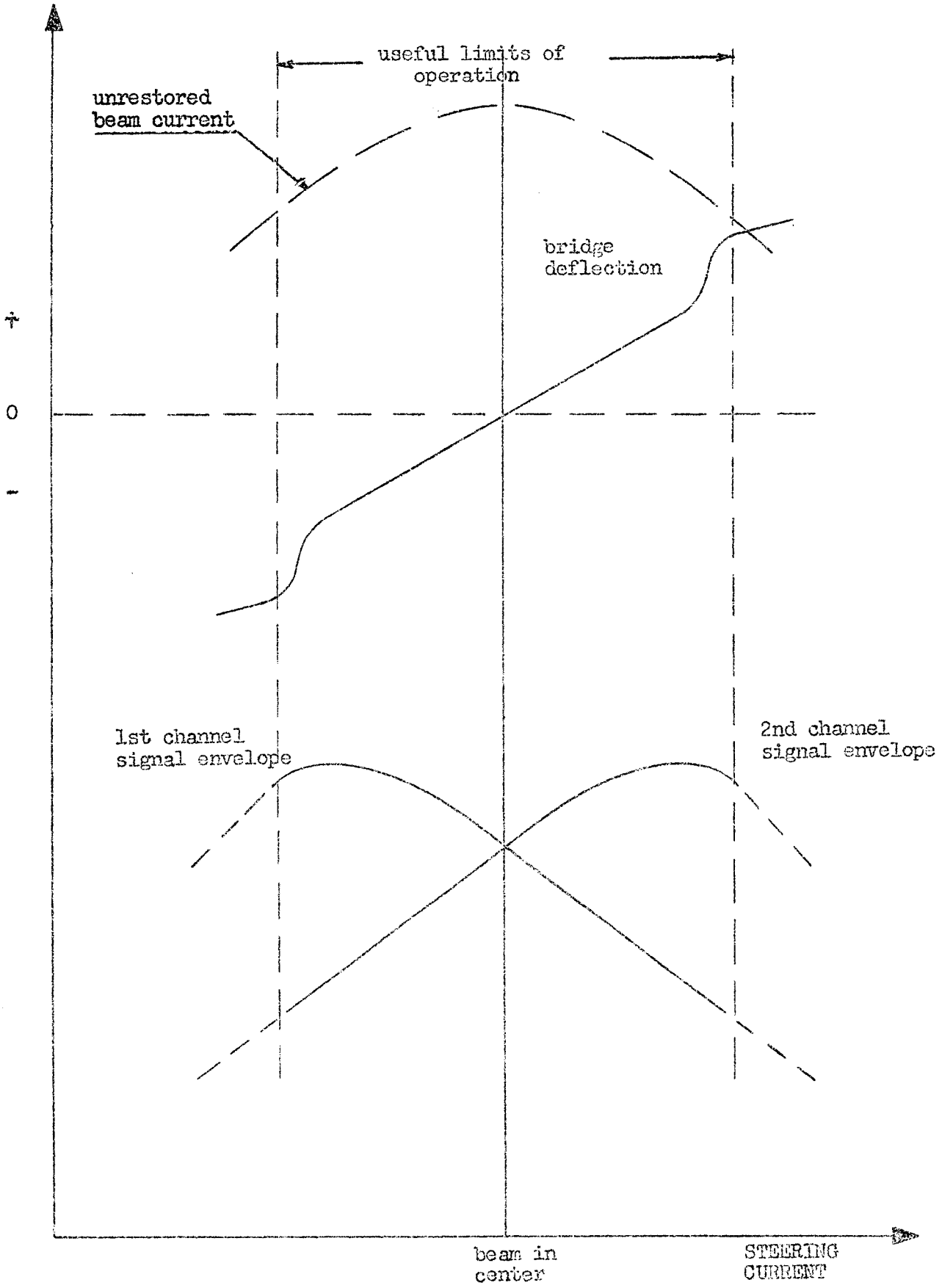

Fig. 6--Beam detector characteristics in case of variable beam intensity.

The probe signals, as displayed on the cathode ray tube, bear traces of the variable beam intensity. They reach a maximum and then, in spite of the fact that the beam is gradually nearing the loops, they have a declining slope. In the central region the two video signals, applied at the input of the circuit under test, yield a deflection indication which is linear. This is due to a good degree of degeneration introduced in the bridge circuit. Beyond this linear tract, both at right and at left, the bridge indications are not usable. This is of little concern because, whatever the means of beam position control will be, the beam is supposed to be back into its (nearly) central position long before it reaches the two useless tracts.

The measurement of the beam intensity by means of the bridge under test, whatever the means of varying it (steering, gun adjustment, etc.), was performed separately. The indications supplied by the bridge, although based only on the use of two loops, were linearly proportional to the indications given by the Faraday cup setup.

The two oscillograms (Figs. 7 and 8) are representative of the signals picked up by the loops, rectified, amplified, and then applied to the bridge. Test conditions are indicated at the side of each oscillogram.

As to the usefulness of a beam position detector, it seems fairly certain that such a device is needed, even if permanent magnetic lenses are used along the accelerator. Misalignment and failure of lens coils are two events that may cause beam displacement. The simultaneous measurement of the beam intensity performed by the detector circuit is an additional useful feature.

5. LABORATORY TEST

The same setup, represented in Fig. 4 but without the pickup loops, has been subjected to a brief laboratory test with a pulse-modulated microwave generator used as signal source. This signal source was feeding a total of 200 mw at 2856 kMc/c into the two bridge channels. In one of these channels a fixed attenuator was included, while the second contained instead a variable attenuator. By varying this latter the ratio of the two signals V_1 and V_2 fed into the two channels was varied. In this manner the actual conditions existing in a drift space, as seen by the two pickup loops, were reproduced.

$$\frac{dp_x}{dt} = e\mu_0 v H_z = e\mu_0 \frac{\pi^2}{a} v \cos \frac{\pi}{a} x \sin \frac{2\pi}{d} z \sin \omega t$$

$$\frac{dp_y}{dt} = eE_y = - ce\mu_0 \frac{\pi}{a} \sin \frac{\pi}{a} x \sin \frac{2\pi}{d} z \cos \omega t$$

$$\frac{dp_z}{dt} = - e\mu_0 v H_x = e\mu_0 \frac{2\pi^2}{ad} v \sin \frac{\pi}{a} x \sin \omega t$$

At the point $x = a/2$ and $z = d/2$,

$$\frac{dp_x}{dt} = 0, \qquad \frac{dp_y}{dt} = 0$$

$$\frac{dp_z}{dt} = e\mu_0 v \frac{2\pi^2}{ad} \sin \omega t$$

$$\Delta p_z = \int_{t_A}^{t_B} e\mu_0 v \frac{2\pi^2}{ad} \sin \omega t \, dt = \int_{t_A}^{t_B} evE_0 \sin \omega t \, dt$$

B. Let us assume that $t_A - t_B$ is short enough so that Δp_z is small compared to p, $\frac{\Delta p_z}{p} \simeq \frac{1}{500}$. In this case the electron can be considered to be moving along $x = a/2$ and $z = d/2$ during the time it is crossing the cavity, and thus $dp_y/dt = 0$ and v is constant during this time.

$$\Delta p_z = \frac{ev}{\omega} E_0 (\cos \omega t_A - \cos \omega t_B)$$

The electrons between -180°, -150° and $+150^\circ$, $+180^\circ$ have to be the ones most deflected, and to be the only ones with such a deflection. Thus by taking $f_0/2$ for the cavity frequency (f_0 being the accelerator frequency) and $\omega t_A - \omega t_B = 30^\circ$:

ωt_A	-120°	-105°	-90°	-60°	-30°	0°	30°	60°	75°	90°	120°
ωt_B	-90°	-75°	-60°	-30°	0°	30°	60°	90°	105°	120°	150°
$\cos \omega t_A - \cos \omega t_B$	.5	.518	.5	.366	.134	-.134	-.366	-.5	-.518	-.5	-.366

and the two curves of the accelerator wave and of the cavity field will be as shown in the following figure.

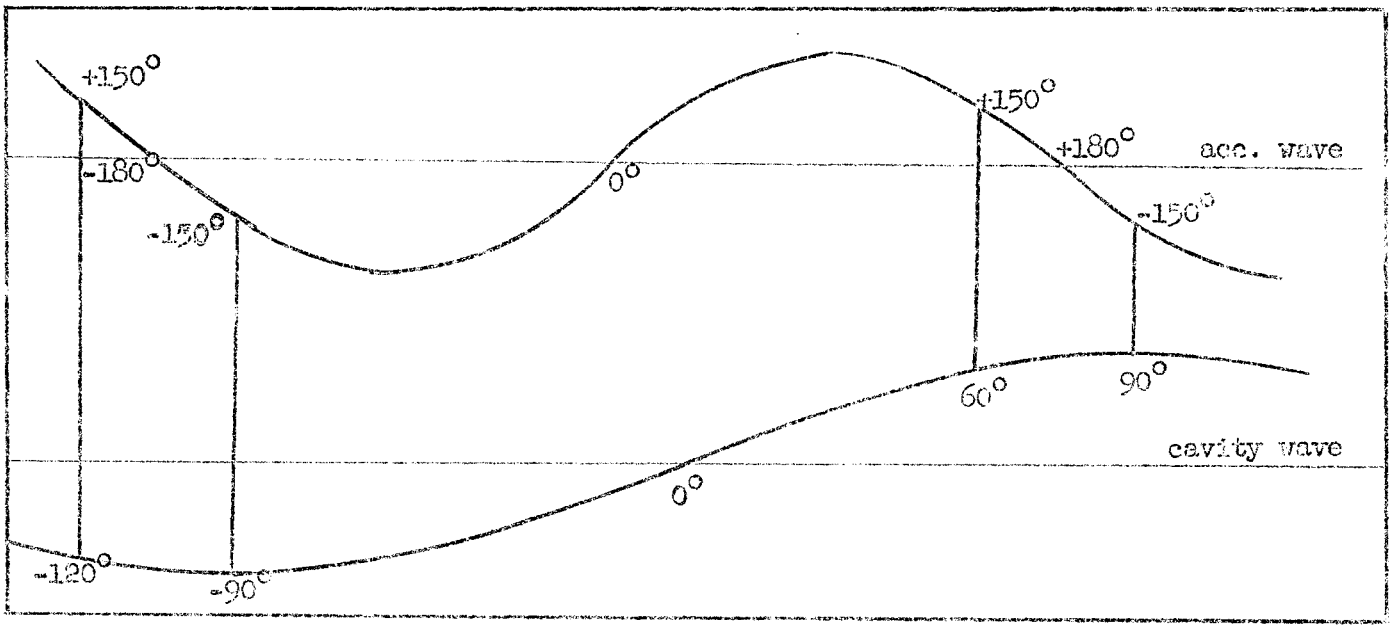

C. After the cavity the electron having Δp_z will be deflected a distance Δr on to the screen located at a distance L.

$$\Delta r = \frac{\Delta p_z}{p} \cdot L$$

In the case where electrons leave the gun with a velocity of 0.5 c,

$$\Delta r = \frac{e}{\omega p_0} .86 E_0 L (\cos \omega t_A - \cos \omega t_B)$$

The test results are represented in Fig. 9. The imperfect linear shape of the curve depicting the dependence of the deviations of the bridge output meter from the ratio V_1/V_2 is mainly due to the nonlinear crystal characteristics. The dissymmetry around the null-balance condition can be attributed to inequalities of the two channels (although an approximate equalization has been reached). The fact that the crystals were unmatched accounts for part of such inequality. As a whole, the curve shape is reasonably good and it can be improved.

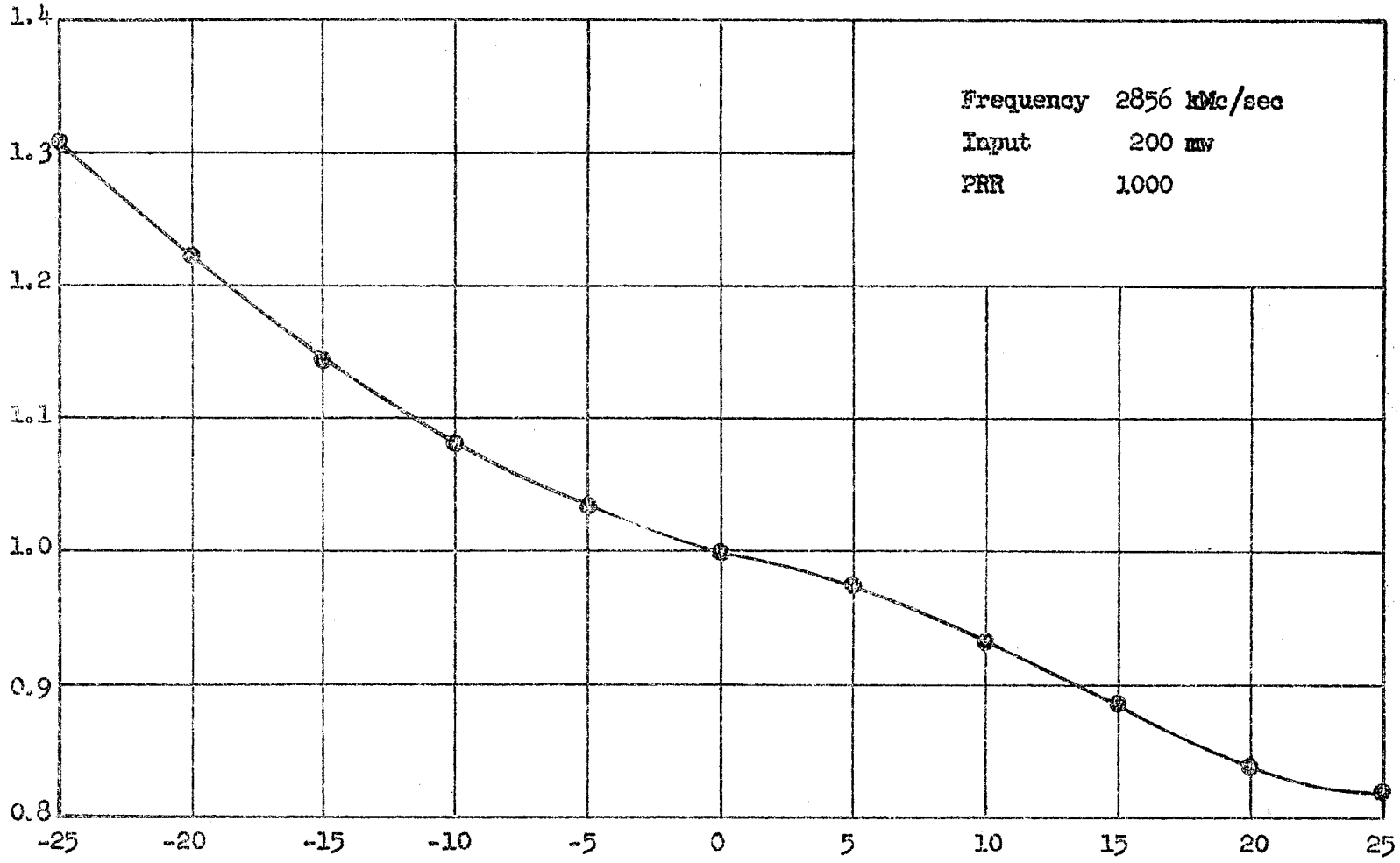

Fig. 9--Meter deflection.